Investigating the Effects of Release Coating on Tool-Part Interaction and Process-Induced Deformations in Composites Manufacturing

Caleb Schoenholz; Navid Zobeiry

DOI: https://doi.org/10.33599/nasampe/s.23.0007

SAMPE publication page

INVESTIGATING THE EFFECTS OF RELEASE COATING ON TOOL-PART INTERACTION AND PROCESS-INDUCED DEFORMATIONS IN COMPOSITES MANUFACTURING

Caleb Schoenholz, Navid Zobeiry
Materials Science & Engineering Department, University of Washington
302 Roberts Hall, Box 352120
Seattle, WA 98195-2120, USA.

ABSTRACT

Although modern-era composites manufacturers possess advanced processing capabilities, several production challenges remain prevalent. One such challenge is mitigating residual stresses and process-induced deformations (PIDs) in composite parts while maintaining a cost-efficient manufacturing workflow. For example, applications and touch-ups of release coatings are labor-intensive process steps and generate high recurring production costs, yet are critical to minimize tool-part interaction and PIDs. One intuitive approach to reduce the frequency of disruptive tool coatings or cleanings may be to apply greater quantities of fresh release coats to a tool surface before completing successive cure cycles. However, the consequential effects of such an approach on tool-part interaction and PIDs are currently undetermined and neglected. This paper first investigates the relationship between release coating quantity and tool surface physicochemical properties using laser microscopy and contact angle goniometry. Then, a novel test fixture installed in a Dynamic Mechanical Analyzer (DMA) is presented and used to quantify tool-part stress developments as a function of fresh release coating quantity applied on a tool surface. Lastly, findings from tool surface characterization and DMA testing were validated by curing long symmetric laminates on tools treated with different release coating quantities in an autoclave and measuring warpages. The results in this paper can be used to expand the current understanding of tool-part interaction and improve the efficiency of tool preparation in composites manufacturing.

Keywords: composites, release coating, tool-part interaction, process-induced deformations
Corresponding author: Navid Zobeiry

1. INTRODUCTION

For decades, fiber-reinforced polymer composites have been increasingly implemented into aerostructures thanks to their efficient strength-to-weight properties. However, although manufacturing technologies have significantly evolved to enable composite-intensive designs, numerous production challenges remain outstanding. One such challenge is mitigating the formation of residual stresses and consequent process-induced deformations (PIDs) in composite parts without significantly disrupting manufacturing throughput [1–4]. During processing, residual stresses and PIDs may be attributed to several micro-, macro-, coupon-, and component-level mechanisms [1]. Some of these mechanisms are well understood and may thus be accurately predicted and efficiently mitigated in industrial settings. However, other contributors remain surrounded by high levels of uncertainty and, therefore, may only be reduced through tacit-based and cost-deficient methods. For example, one source of high uncertainty is the effects of release coating on the interfacial bonding and friction between a tool and composite part during processing (i.e., tool-part interaction) [5–15].

During autoclave processing of large aerostructures, tool surfaces are typically treated with release coatings prior to part lay-up to reduce tool-part interaction and PIDs, and facilitate the demolding of cured parts [16–20]. Aerospace manufacturers typically use semi-permanent, silicone-based release coatings for autoclave processing, such as Loctite® Frekote® 710-NC™ [21]. Frekote products may be sprayed, wiped, rolled, or brushed onto tool surfaces as liquids and cured through an evaporation reaction to form a thin abhesive (i.e., non-stick) layer. Once all the applied release coats are sufficiently cured, the composite material is laid up on the tool, vacuum bagged, and loaded into an autoclave. Next, external pressures and temperatures (e.g., 7 atm and 180 °C for thermosets) are applied to stimulate the cross-linking reaction and transform the composite material into a solid structure. In addition to the formation of interfacial physicochemical bonds, autoclave pressures and temperatures may also create free strain mismatches between the tool and part due to thermal expansion differences and cure shrinkage in the composite. When combined with interfacial bonds, these free strain mismatches create a shear interaction at the tool-part interface that transfers stresses through the release coating and into the tool-adjacent composite plies. Some of these stresses are alleviated in plies furthest away from the tool surface through interlaminar shear. However, some stresses remain unrelieved and become locked-in as curing progresses, resulting in a through-thickness residual stress gradient in the composite part. As the thermoset composite undergoes a cross-linking polymerization reaction, some silicone molecules in the release coating also transfer from the tool to the part's surface and become physically and chemically integrated into its resin network [19,22]. During the demolding process after the cure cycle, the locked-in stress gradient is partially released through bending deformation, while the silicone molecules remain on the cured part's tool-side surface. This common scenario results in the warpage and contamination of an initially flat laminate, as schematically shown in Fig. 1.

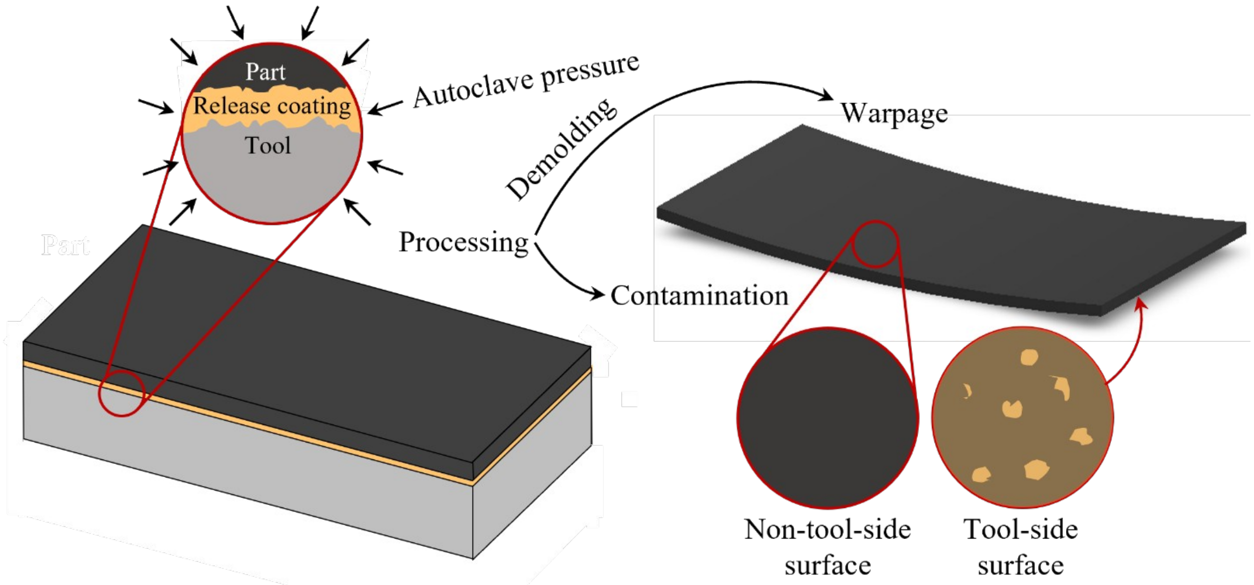

Figure 1. Schematic of tool-part interaction during autoclave processing and the resulting warpage and contamination of an initially flat laminate.

Although the general mechanisms of tool-part interaction and PIDs are reasonably well understood, several contributing variables remain with high levels of uncertainty. For example, the relationship between fresh Frekote release coating quantity on a tool surface, tool-part interfacial stress developments, and PIDs is undetermined. This is partly due to a lack of an established test method for accurately measuring the degree of tool-part interaction during composites processing. As a result, manufacturers rely on know-how during tool preparation steps and, rather than conduct periodic touch-ups, may apply excessive amounts of fresh release coating before successive processing cycles. This intuitive approach would decrease the possibility of permanent tool-part bonding and tool damage, lower the rate of aging in the release coating, and reduce the frequency of tool cleanings and touch-ups needed throughout the processing campaign [16–18]. However, excessive use of fresh release coating may have undesirable consequences on tool-part interaction and PIDs since the maximum performance of Frekote products occurs after the coating has undergone several processing cycles [16,21]. Neglecting these potential effects of release coating thus restricts the controllability of PIDs and forces manufacturers to use compensation methods during assembly (e.g., shimming) to meet geometric tolerances. Unfortunately, in addition to cost considerations, such assembly compensation methods may introduce further residual stresses in parts and consequently reduce structural efficiency.

This paper investigates the impact of fresh release coating quantity on tool surface physicochemical properties, tool-part interaction, and PIDs. First, tool surface features, roughness, and free energy are characterized as a function of Frekote 710-NC release coats using laser scanning digital microscopy and contact angle goniometry. Then, a custom-built technique installed in a Dynamic Mechanical Analyzer (DMA) to directly measure interfacial stresses and characterize tool-part interaction during processing cycles is presented. In this study, the novel technique is used to investigate the effects of release coat quantity on tool-part interfacial stress development for an aerospace-grade material system. The characterized tool surface properties and interfacial stresses are then validated by fabricating long and symmetric laminates using similar surface conditions as DMA tests and measuring process-induced warpages. The results of this study are intended to expand the current understanding of release coating and tool-part interaction, improve the efficiency of tool preparation, and potentially mitigate PIDs in composites processing.

2. EXPERIMENTATION

2.1 Materials

The release coating used in this study was Loctite® Frekote® 710-NC™ release agent (RA). The exact formulations of Frekote products are proprietary, but some information of 710-NC is listed on its publicly available datasheet [21]. The composition by weight of Frekote 710-NC includes 1-5 % silicone components (reaction product of TMAS and PDMS), 1-5 % octane, 1-5 % hydrocarbons (C7-10), 60-100 % petroleum as the carrier, and 10-30 % dibutyl ether as the solvent. After the release coating is applied on a tool, most of the carrier and solvent evaporate, while the silicones and hydrocarbons remain on the lay-up surface [16].

The composite material used in this study was Toray T800S/3900-2 UD prepreg with a resin content of 35 % by weight [23]. 3900-2 is a toughened aerospace-grade epoxy resin, while T800S is an intermediate-modulus and high-strength carbon fiber. In addition to epoxy resin, the prepreg's surface and interlayer regions are partially covered with micro-spherical thermoplastic tougheners. In recent decades, the T800/3900-2 system has been used as a primary structural material on major aircraft such as the Boeing 787 [24].

2.2 Methods

2.2.1 Tool Surface Tests

The first experimental phase consisted of treating tools with different amounts of release coating, then conducting digital microscopy and contact angle goniometry to characterize the resulting physicochemical properties. First, ten flat laboratory-scale (i.e., coupon-sized) tools were made by cutting 12.7 mm (w) × 25.4 mm (l) sections from a 0.127 mm (t) C1095 spring steel feeler gage with an ISO 1302 surface roughness grade of N3 [25,26]. Next, all ten tools were cleaned with Loctite® Frekote® PMC™ mold cleaner [27] and a lint-free cotton wiping cloth to remove any surface residue from previous cutting and handling. Then, various quantities of Frekote 710-NC RA were applied to the tool surfaces using a lint-free cotton wiping cloth, allowing 15 minutes between coats and after the final coat as recommended on the product's datasheet [21]. Two tools were treated with zero coats (i.e., untreated), two were treated with one coat, two were treated with two coats, two were treated with three coats, and two were treated with four coats of Frekote 710-NC RA.

After all the release coats were sufficiently cured, one tool with each surface condition (i.e., zero, one, two, three, or four layers of RA) was analyzed using an Olympuvaris LEXT OLS4100 laser scanning digital microscope at 100x magnification. The OLS4100 was used to generate non-contact height maps and calculate the arithmetical mean height (Sa) in three different areas for each tool surface condition. Lastly, contact angle goniometry tests were performed on the other half of the prepared tools using an AST Optima Video Contact Angle (VCA) System. Five 1-μl droplets of deionized (DI) water and diiodomethane (DIM) were dispensed on each tool using the

VCA's motorized syringe. Side-view images and contact angles of each droplet were obtained immediately after solid-liquid contact using the VCA system. The five DI water and DIM contact angles were used in conjunction to create 25 polar-dispersive contact angle pairs for each surface condition. Using the Owens-Wendt method [28], these contact angle pairs were then used for 25 surface free energy (SFE) calculations on each tool treated with different amounts of release coating.

2.2.2 Tool-Part Interaction Tests

The second experimental phase involved creating two cross-ply composite laminates and measuring tool-part interfacial stresses during processing using a custom DMA fixture. First, ten plies of T800S/3900-2 with nominal dimensions of 4 mm (w) × 4 mm (l) were cut using an X-ACTO® knife. The plies were then stacked to create two cross-ply laminates, each with a $[90/0/\overline{90}]_s$ layup. Next, both laminates were simultaneously hot-debulked for 30 minutes at 60 °C on a hotplate under approximately 0.7 MPa (~7 atm.) of applied pressure from caul plates. The laminates were then removed from the hot plate and cooled down to room temperature before testing in the DMA.

Fig. 2 shows an image of the custom fixture built to measure interfacial shear stresses during composites processing. The setup was constructed using the shear sandwich clamp in a TA Instruments® Discovery Dynamic Mechanical Analyzer (DMA) 850, and custom-machined U- and C-shape tools to cover the moveable and stationary clamps. All custom tools were made from A2 tool steel with an ISO 1302 surface roughness grade of N3 (i.e., comparable to the tools used during tool surface tests). The U-shape tool was reused throughout the entire testing campaign, while two new C-shape tools were prepared for each DMA test using a manual shear/brake combination machine.

Before each test, the U-shape tool was cleaned with Loctite® Frekote® PMC™ mold cleaner [27] to remove any surface residue from previous testing and handling. Then, each outside surface on the U-shape tool was treated with either one, two, three, or four layers of Frekote 710-NC RA using a lint-free cotton wiping cloth, allowing 15 minutes between coats as recommended on the product's datasheet [21]. The outside surfaces of the C-shapes were roughened using 80 grit aluminum oxide sandpaper for two minutes. The abraded surfaces were then cleaned with isopropyl alcohol (IPA) to remove any steel dust created during sanding. After all custom tools were prepared and secured over the DMA clamps, the composite laminates were sandwiched between the U- and C-shapes with the 90° plies facing horizontally. Approximately 0.7 MPa of compaction pressure was applied to the laminates using the knurled knobs and monitored throughout the cure cycle by placing FlexiForce™ HT201 piezoresistive force sensors [29] between each stationary clamp and C-shape tool.

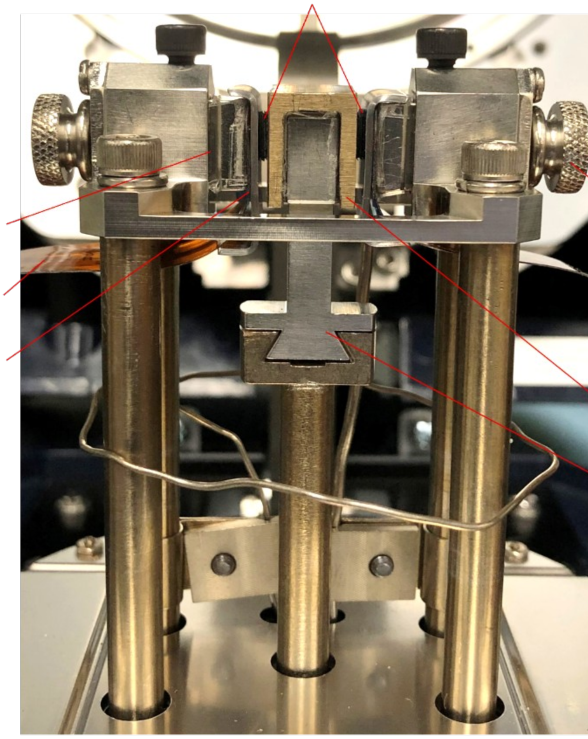

Figure 2. Custom DMA shear test setup used to measure tool-part interfacial stresses during composites processing cycles.

Once the composite laminates were loaded into the DMA shear sandwich fixture, the system was subjected to a temperature cycle following the Manufacturer's Recommended Cure Cycle (MRCC) [23]. The temperature cycle consisted of heating to 180 °C at 2 °C/min, holding at 180 °C for 120 minutes, then cooling the system down. As previously mentioned, four different tool surface conditions were applied to the moveable U-shape tool throughout the testing campaign: one, two, three, or four layers of Frekote 710-NC RA. The zero-coat surface condition was neglected in DMA tests to avoid permanent tool-part bonding and potential tool damage during testing. Two tests were conducted for each surface condition for a total of eight tests.

During the heat-up stage of the cure cycle, the laminates begin to cure, and the outwards-facing plies form strong primary bonds and mechanical bonds with the abraded C-shape tool surfaces. The composites thus remain bonded and fixed to the stationary C-shapes throughout the test. The inwards-facing plies of the laminates form weaker primary and secondary bonds with the U-shape tool since its surfaces are covered with release coating. The laminates are held stationary during cure until their gel points, where tool-part stresses start to evolve [8,9]. Gelation was estimated to occur 90 minutes into the cure cycle based on previous studies [2]. Upon gelation, an upwards force was applied from the DMA drive motor to generate vertical motion in the U-shape tool. This motion created a constant tool-part shear strain mismatch, which was applied through the remaining time of the 180 °C temperature hold. Due to equipment limitations of the DMA, the strain rate could not be applied during cool-down, and thus the cooling stage of the cure cycle was neglected in this study. As previously mentioned, the composite samples remained stationary throughout the cure cycle as they were strongly bonded to the outside C-shape tools. A constant displacement rate of 0.05 mm/min was chosen for all DMA tests based on a previous study by Ersoy et al. [9]. The DMA automatically measured and recorded forces needed to produce the tool-part shear strain throughout the cure cycle. The recorded forces were then divided by the effective sample area to calculate tool-part interfacial shear stresses.

2.2.3 Warpage Tests

The final experimental phase was conducted to validate tool surface characterizations and DMA tests. To achieve this, long and symmetric composite parts were cured in an autoclave on tools covered with different amounts of release coating, and the parts' post-demolding warpages were measured. Two parts were processed for each release coating quantity to account for and evaluate material, process, and tool surface variabilities. Standard prepreg lay-up and vacuum bagging procedures were used to fabricate the composite parts. First, a flat plate made of A2 tool steel with an ISO 1302 surface roughness grade of N3 (i.e., comparable to the tools used during tool surface and DMA tests) was treated with Frekote 710-NC release agent using a lint-free cotton wiping cloth. The tool surface was cleaned with PMC mold cleaner and retreated with 710-NC before each test. Then, four 90-degree plies of T800S/3900-2 prepreg with nominal dimensions of 80 mm (w) × 400 mm (l) were cut using an X-ACTO® knife. The plies were then stacked adjacently on the tool surface to create two $[90]_2$ laminates. Next, the tool and composite laminates were covered with one sheet of fluorinated ethylene propylene (FEP) release film. Separate steel caul plates were then placed on top of the FEP directly over the laminates to ensure volume fraction symmetry in the parts. FEP between the caul plates and laminates acted as a barrier to restrict any interfacial adhesive bonding between the top surfaces of the parts and the caul plates. The tool and lay-ups were then covered by one layer of breather cloth, sealed in vacuum bagging, loaded into an autoclave, and subjected to the MRCC. Four different quantities of release coating were used for the autoclave processing cycles: one, two, three, and four layers. After a cure cycle was completed, the composite parts were demolded, placed on their longitudinal sides, and the maximum warpages were measured using a Keyence LJ-X8400 2D laser profiler.

3. RESULTS

3.1 Tool Surface Test Results

Fig. 3 shows three-dimensional height maps of steel tools covered with zero to four coats of Frekote 710-NC RA. The figure reveals distinct surface features on tools treated with different amounts of release coating. For example, the steel tool treated with one release coat has a similar height profile and grain visibility to the untreated zero-coat tool. This suggests that one 710-NC release coat may be insufficient to cover significant tool surface irregularities (e.g., grains, cavities, scratches) that would otherwise promote tool-part interaction [15]. On the other hand, the tools treated with two, three, and four release coats demonstrate a mitigation of most tool surface irregularities. In addition to an increase in overall coating thickness, the two-, three-, and four-coat micrographs show that each additional application of release coating results in an increased number and size of agglomerations (i.e., bumps) on the tool surfaces. These micro-agglomerations form when a fresh coat of 710-NC is applied on top of a low-energy surface, such as another cured release coating layer [30]. Such agglomerations may significantly affect a tool's physicochemical properties, tool-part interaction, and PIDs [15,31].

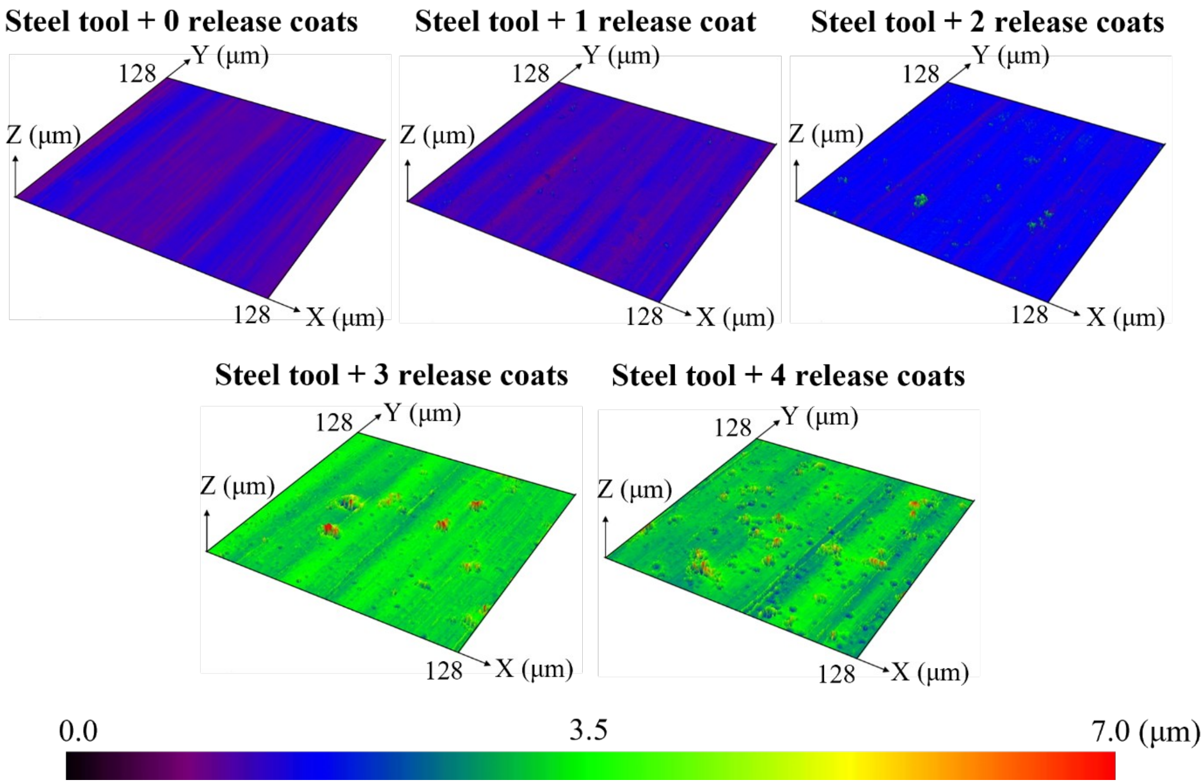

Figure 3. Three-dimensional height maps of steel tools treated with different numbers of Frekote 710-NC release coats.

Fig. 4 shows the surface roughness (i.e., arithmetical mean height, Sa) and SFE (σ_{tool}) of steel tools treated with zero to four 710-NC release coats. The surface roughness and SFE values reported in the plot are averages from three and twenty-five measurements, respectively. Error bars in the figure represent the standard deviation (SD) or scatter within each measurement set. The plot demonstrates distinct physicochemical variations between tools treated with different quantities of fresh release coating. For example, the figure illustrates that applying one release coat to an uncoated steel tool slightly lowers its surface roughness from approximately 0.12 to 0.11 μm. This reduction suggests that one coating layer may fill in at least some tool surface irregularities and create a smoother lay-up surface. In addition to reducing roughness, one release coat also significantly decreased the tool's SFE from approximately 32 to 19 mJ/m^2. This exceptionally low SFE value indicates Frekote 710-NC is highly abhesive (i.e., non-adhesive) and is thus an ideal coating to reduce tool-part chemical bonding during processing.

After the one-coat measurements, tool surface roughness increased drastically with each additional layer due to a greater extent and size of coating agglomerations. Although elevated pressures and temperatures likely cause Frekote agglomerations to behave rubbery during autoclave processing, an increase in tool surface roughness is typically associated with elevated levels of tool-part interaction and PIDs [15]. In addition to surface roughness, average SFE values increased slightly with each applied release coat but remained exceptionally low. These measurements suggest that the level of chemical bonding between a composite part and a release-coated tool surface would be relatively insensitive to the number of coats applied before processing. The SD values (i.e., error bars) of surface roughness and SFE measurements also increased with each additional release coat. The notably larger scatter in measurements on tools treated with higher numbers of release coats was likely due to a greater amount of non-uniform agglomerations [30,32].

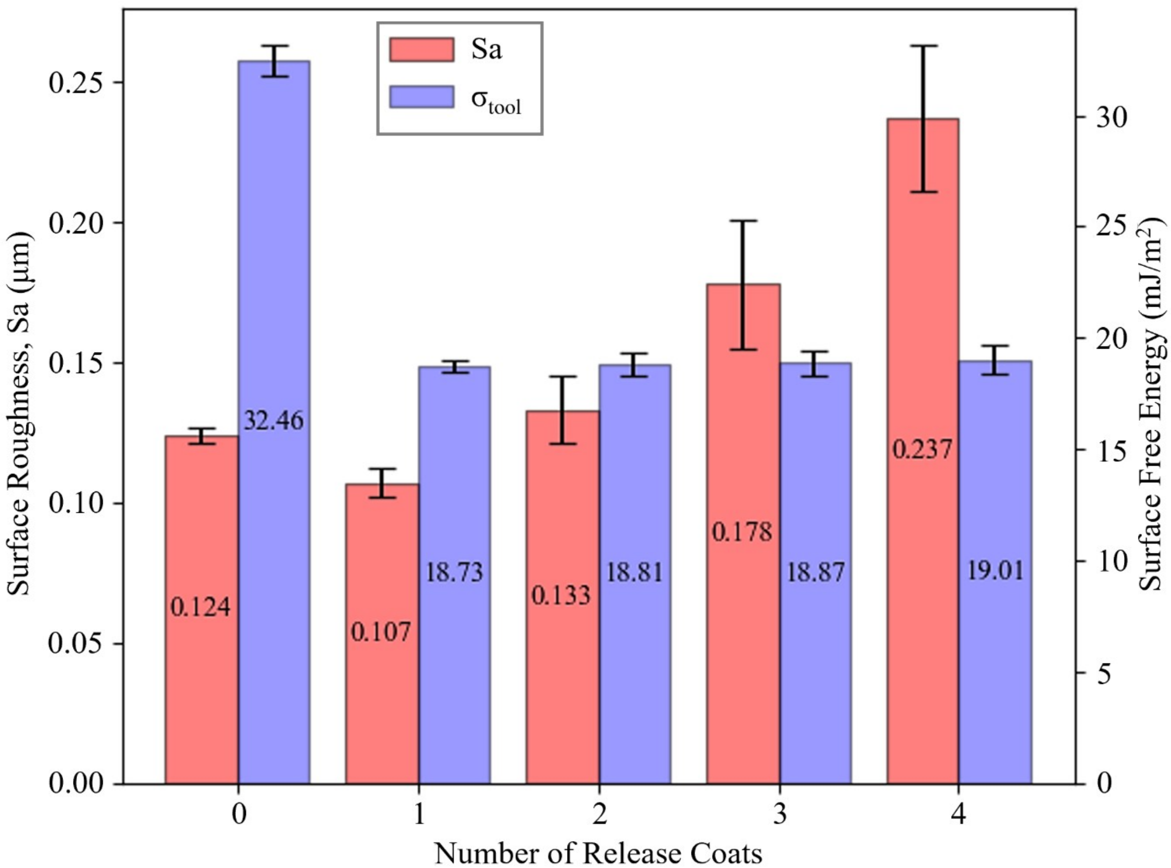

Figure 4. Surface roughness (Sa) and surface free energy (σ_{tool}) of steel tools treated with different numbers of Frekote 710-NC release coats.

3.2 Tool-Part Interaction Test Results

Fig. 5 shows the development of tool-part interfacial stresses ($\tau_{tool\text{-}part}$) throughout the MRCC of T800S/3900-2. During the test, the moveable U-shape tool was covered with three coats of Frekote 710-NC, as recommended on the product's datasheet [21]. The temperature profile (T), simulated glass transition temperatures of thermoset resin and thermoplastic particles ($T_{g.ts}$ and $T_{g,tp}$, respectively), and degree of cure (DoC) are also shown in the graph. Tool-part stresses were confined at zero until the strain rate was applied at the gel point 90 minutes into the cure cycle. Upon gelation, tool-part stresses evolved linearly, reached a maximum value, sharply dropped, then decreased non-linearly through the remainder of the isothermal hold at 180 °C.

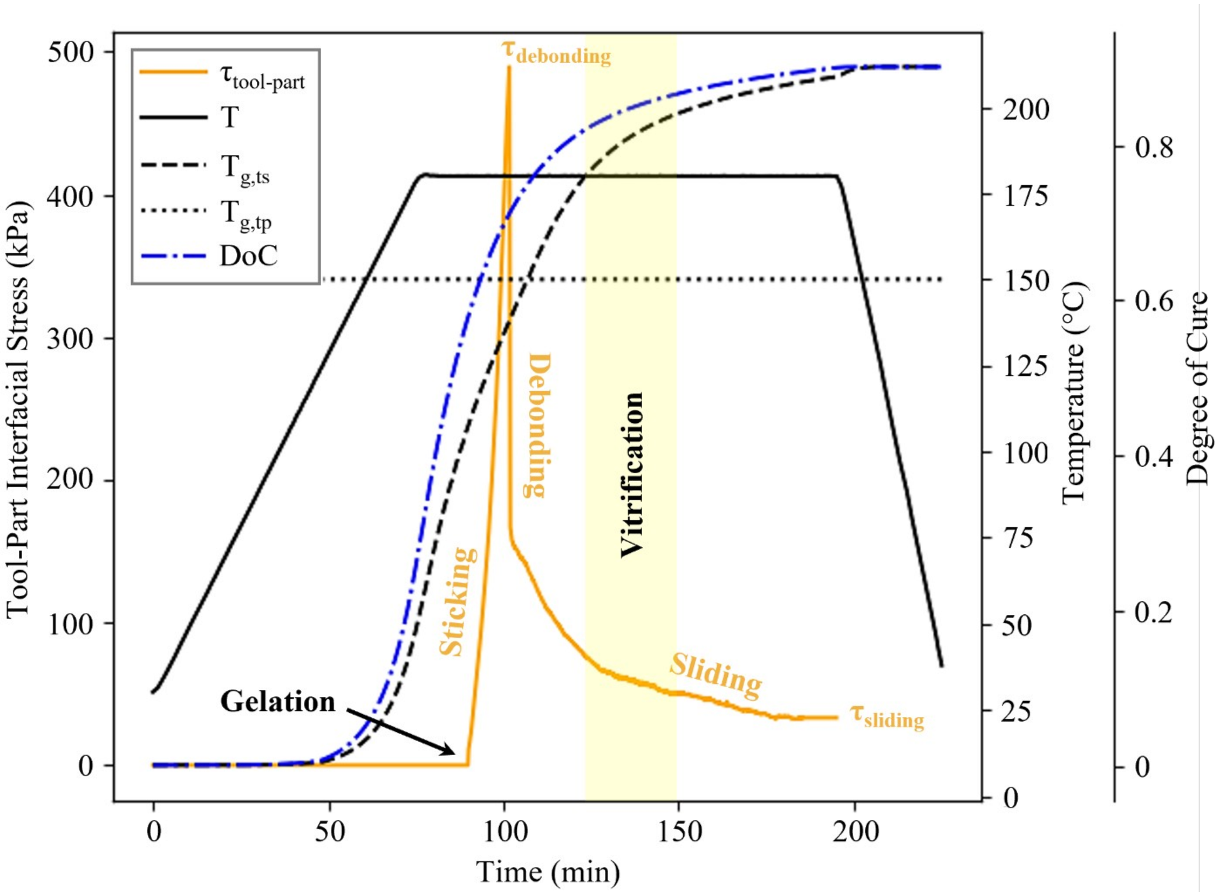

Figure 5. Tool-part interfacial stress ($\tau_{tool\text{-}part}$) development between T800S/3900-2 laminates with $[90/0/\overline{90}]_s$ layups and a steel tool covered with three Frekote 710-NC release coats.

The initial rise in stress upon gelation represents sticking (i.e., static friction) between the tool and part [8,9,11]. At this stage of the cure cycle, the resin has transformed from a viscous fluid to a rubbery solid. Since the processing temperature at gelation is well above the glass transition temperature of the thermoplastic particles, these components are also in a rubbery state [33]. The friction between a rubbery solid and a hard surface (e.g., a tool) is mainly controlled by two mechanisms: interfacial adhesion and internal viscoelastic deformations. As previously mentioned, resistive mechanical forces also contribute to friction between any two solid bodies but may be considered negligible when one of the solids is a soft rubber [31]. Interfacial adhesion directly results from SFE effects causing the polymer chains in the rubbery material to form adhesive bonds and become “pinned” to the hard surface. On the other hand, internal viscoelastic contributions arise due to friction between polymer chains in the bulk of the rubber. When subjected to normal pressure and in-plane strain, such as in the DMA setup, oscillating forces are exerted on the rubbery material. These forces lead to energy dissipation via internal viscoelastic mechanisms of the rubber’s polymer chains [31]. Since Frekote 710-NC RA with exceptionally low SFE properties (i.e., 19 mJ/m^2) was applied to the tool before processing, strong interfacial adhesive bonds are unlikely to form during the cure cycle. Therefore, the linear increase in stress upon gelation was primarily due to internal strain resistive viscoelastic friction in the composite’s resin and thermoplastic particles, given that both components were in the rubbery regime.

Mechanical friction between the tool and any exposed fiber surfaces may also potentially contribute to this stress.

After approximately ten minutes (i.e., 0.5 mm) of applied strain, interfacial stresses reached a maximum value of 489 kPa before sharply dropping. This ultimate stress value is often referred to as the tool-part debonding stress ($\tau_{debonding}$) and signifies the transition from static to kinetic friction. Fig. 5 illustrates that debonding occurred while the resin and thermoplastic particles were still in their rubbery states. A broken tool-part bond at this stage of the cure cycle may thus be described as the polymer chains on the composite part's surface undergoing a rapid "snapping" or "unpinning" from the tool [31]. The post-debonding regime in Fig. 5 shows a sharp drop in stress to an intermediate value of approximately 150 kPa, then a non-linear decline through the remainder of the isothermal hold. The gradual stress decay represents sliding or kinetic friction between the tool and part [8,9,11]. Immediately after tool-part debonding occurred, the glass transition temperature of the resin was rapidly evolving and approaching the processing temperature. However, the thermoplastic particles' glass transition temperature remained constant and below 180 °C until the end of the cure cycle. In other words, the composite's resin was transitioning from a rubbery viscoelastic body to a glassy elastic solid, while the thermoplastic particles remained in their rubbery state. The resin's transition to an elastic solid would consequently be accompanied by a reduction of the viscoelastic friction contributions and, thus, a direct decline in overall sliding stress values, shown in Fig. 5.

Upon reaching the vitrification zone, the thermoset resin begins acting like an elastic solid, and the dominant strain-resistive contribution shifts to mechanical friction with the tool [11,34]. Mechanical friction may be considered elastic resistance to deformation from material asperities at the tool-part interface during the applied strain. At the end of the isothermal hold, the thermoset resin is a fully elastic solid, and its viscoelastic contributions to friction are minimal. The final sliding stress value of approximately 30 kPa was thus primarily determined by mechanical friction in the thermoset resin and internal viscoelastic effects in the thermoplastic particles.

Fig. 6 shows tool-part interfacial stress versus strain throughout the MRCC for four tool surface conditions ranging from one to four coats of Frekote 710-NC. The profiles shown in solid lines represent the first DMA test conducted at each pressure, while dashed curves correspond to duplicate tests. The plot only includes stress developments through the end of the thermoset's vitrification zone to illustrate discrepancies between tests more clearly. In all eight trials, the applied strain at gelation caused sharp linear increases in stress. These results indicate that a tool and composite part exhibit sticking behavior regardless of the number of release coats. All stress profiles then progressed to maximum values where debonding occurred within a narrow window of 70-74% degree of cure. After debonding, all stress profiles showed non-linearly decaying sliding regimes in response to vitrification and the transition to mechanical friction forces.

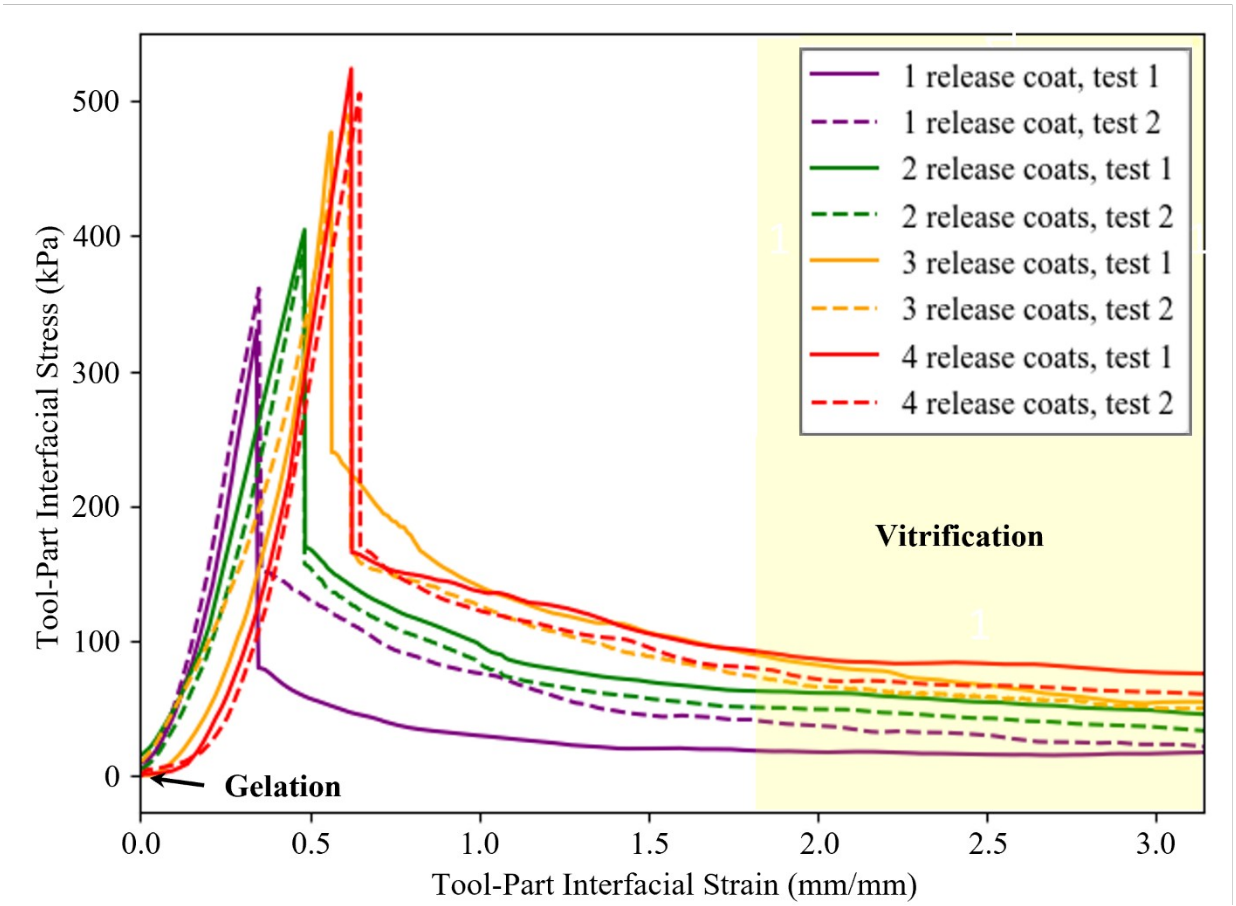

Figure 6. Tool-part interfacial stress developments between T800S/3900-2 laminates with $[90/0/\overline{90}]_s$ layups and a steel tool covered with different numbers of Frekote 710-NC release coats.

The magnitudes of debonding stresses ($\tau_{debonding}$) and sliding stresses ($\tau_{sliding}$) demonstrated a direct increase with the number of release coats and pre-processing tool surface roughness (Sa), as shown in Fig. 7. These results support Amontons' first law, which states that friction (e.g., tool-part stress) between two rigid bodies is mechanically-driven and thus directly proportional to surface roughness [34]. Although the composite laminates were in rubbery states when debonding occurred for all tests, differences in bulk viscoelastic contributions were likely marginal since processing conditions were kept constant. Therefore, the discrepancies in tool-part stress developments were likely caused by the U-shape tool's surface condition (i.e., roughness) and resulting mechanical forces.

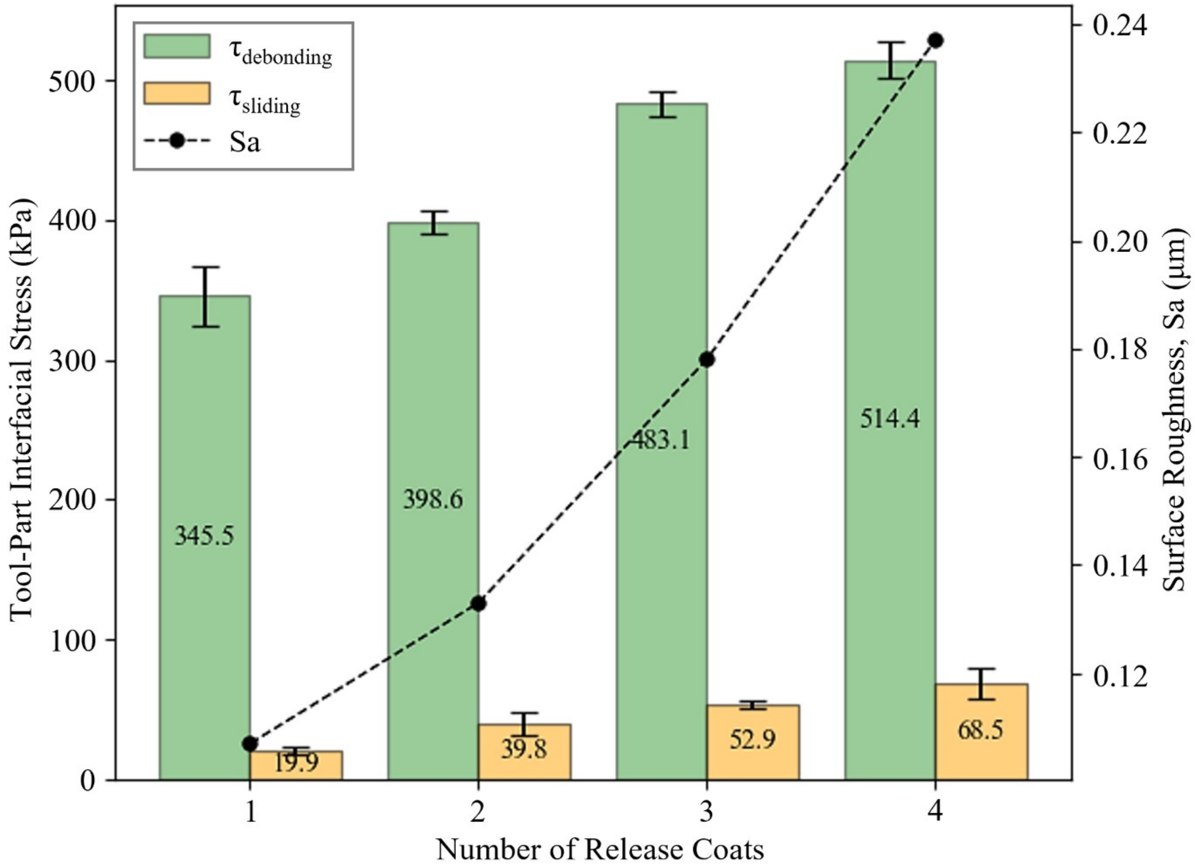

Figure 7. Tool-part debonding stress ($\tau_{debonding}$), sliding stress at the end of vitrification ($\tau_{sliding}$), and surface roughness (Sa) between T800S/3900-2 laminates with $[90/0/\overline{90}]_s$ layups and a steel tool covered with different numbers of Frekote 710-NC release coats.

3.3 Warpage Test Results

Fig. 8 shows warpage magnitudes of the $[90]_2$ laminates cured on four tool surface conditions ranging from one to four coats of Frekote 710-NC. Tool-part debonding and sliding stresses from DMA tests are also shown in the plot. The averages of two experimental measurements for each condition are displayed as points, and trendlines were fitted to the data for illustration purposes only. Error bars in the figure represent the standard deviation (SD) or scatter within each measurement set. Warpage values ranged from approximately 4.5 to 8 mm, with the highest value occurring from the tool surface treated with four release coats. As previously mentioned and shown in Fig. 7 and Fig. 8, similar trends were measured for debonding and sliding stresses in the DMA. These results indicate that the excessive application of fresh release coating increases levels of tool-part stress and the warpage of flat symmetric laminates for a tool's first processing cycle. In other words, if only completing one processing cycle, manufacturers should treat tools with conservative amounts of release coating (i.e., only enough to restrict permanent tool-part bonding) to reduce PIDs. If completing a series of several processing cycles, the effects of release coating aging on tool-part stress developments and PIDs must also be considered. Such effects are outside the scope of this paper and will be investigated in a future study.

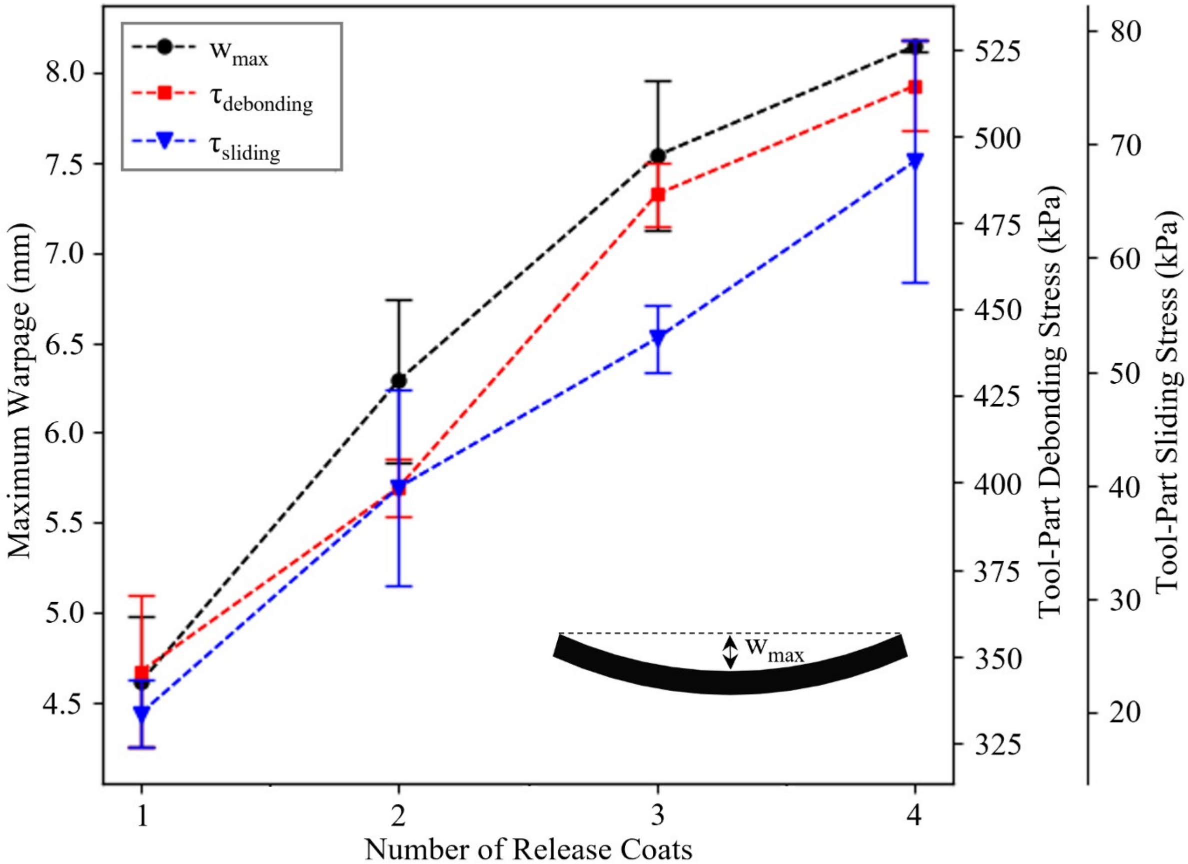

Figure 8. Maximum warpage (w_{max}) of $[90]_2$ composite parts cured in an autoclave, and tool-part debonding and sliding stresses ($\tau_{debonding}$, $\tau_{sliding}$) measured during DMA testing for steel tools treated with different numbers of Frekote 710-NC release coats.

4. CONCLUSIONS

The main objective of this study was to investigate the effects of release coating on tool-part interaction and PIDs for Toray T800S/3900-2. To achieve this goal, tool surface roughness and surface free energy were characterized as a function of Frekote 710-NC release coats using laser microscopy and contact angle goniometry. Then, a custom DMA shear test setup was presented and utilized to characterize the development of tool-part interfacial stresses throughout a cure cycle for different quantities of release coating. Lastly, the warpage values of flat laminates cured on tools with similar surface conditions as DMA tests were used to validate tool-part stress measurements. The main conclusions from this work are as follows:

- A significant relationship exists between the number of release coats and a tool's physicochemical properties. Tool surface roughness increases considerably with each additional release coat applied due to increased levels of coating agglomerations. Tool surface free energy is at most marginally affected by the number of release coats.

- Tool-part interfacial stresses for T800S/3900-2 are directly affected by the number of fresh release coats applied to a tool surface. The highest tool-part debonding and sliding stresses occur when composite parts are processed on tools treated with excessive amounts of release coating (i.e., four coats). Conversely, the lowest tool-part stresses occur on tools treated with only one release coat. The direct relationship between tool-part stress magnitudes and the number of release coats is likely due to mechanical interactions occurring at the tool-part interface.

- The warpage of flat $[90]_2$ T800S/3900-2 parts shows similar trends as tool-part interfacial stresses, with the highest values occurring on tools with the greatest number of release coats and highest pre-processing surface roughness. Maximum warpage of flat composite parts may be directly related to the tool-part debonding and sliding stresses.

5. ACKNOWLEDGEMENTS

This work was supported by Toray Composite Materials America, Inc. Part of this work was conducted at the Washington Clean Energy Testbeds, a facility operated by the University of Washington Clean Energy Institute.

6. REFERENCES

[1] Zobeiry N, Poursartip A. The origins of residual stress and its evaluation in composite materials. Structural Integrity and Durability of Advanced Composites: Innovative Modelling Methods and Intelligent Design 2015:43–72. https://doi.org/10.1016/B978-0-08-100137-0.00003-1.

[2] Zobeiry N, Forghani A, Li C, Gordnian K, Thorpe R, Vaziri R, et al. Multiscale characterization and representation of composite materials during processing. Philosophical Transactions of the Royal Society A: Mathematical, Physical and Engineering Sciences 2016;374. https://doi.org/10.1098/RSTA.2015.0278.

[3] Fernlund G, Mobuchon C, Zobeiry N. 2.3 Autoclave Processing. Elsevier; 2018. https://doi.org/10.1016/B978-0-12-803581-8.09899-4.

[4] Li C, Zobeiry N, Keil K, Chatterjee S, Poursartip A. Advances in the Characterization of Residual Stress in Composite Structures. SAMPE 2014 - SEATTLE, 2014.

[5] Twigg G, Poursartip A, Fernlund G. Tool–part interaction in composites processing. Part I: experimental investigation and analytical model. Compos Part A Appl Sci Manuf 2004;35:121–33. https://doi.org/10.1016/S1359-835X(03)00131-3.

[6] Twigg G, Poursartip A, Fernlund G. Tool–part interaction in composites processing. Part II: numerical modelling. Compos Part A Appl Sci Manuf 2004;35:135–41. https://doi.org/10.1016/S1359-835X(03)00132-5.

[7] Potter KD, Campbell M, Langer C, Wisnom MR. The generation of geometrical deformations due to tool/part interaction in the manufacture of composite components. Compos Part A Appl Sci Manuf 2005;36:301–8. https://doi.org/10.1016/J.COMPOSITESA.2004.06.002.

[8] Twigg G, Poursartip A, Fernlund G. An experimental method for quantifying tool–part shear interaction during composites processing. Compos Sci Technol 2003;63:1985–2002. https://doi.org/10.1016/S0266-3538(03)00172-6.

[9] Ersoy N, Potter K, Wisnom MR, Clegg MJ. An experimental method to study the frictional processes during composites manufacturing. Compos Part A Appl Sci Manuf 2005;36:1536–44. https://doi.org/10.1016/J.COMPOSITESA.2005.02.010.

[10] Zappino E, Zobeiry N, Petrolo M, Vaziri R, Carrera E, Poursartip A. Analysis of process-induced deformations and residual stresses in curved composite parts considering transverse shear

stress and thickness stretching. Compos Struct 2020;241:112057. https://doi.org/10.1016/J.COMPSTRUCT.2020.112057.

[11] Kaushik V, Raghavan J. Experimental study of tool–part interaction during autoclave processing of thermoset polymer composite structures. Compos Part A Appl Sci Manuf 2010;41:1210–8. https://doi.org/10.1016/J.COMPOSITESA.2010.05.003.

[12] Albert C, Fernlund G. Spring-in and warpage of angled composite laminates. Compos Sci Technol 2002;62:1895–912. https://doi.org/10.1016/S0266-3538(02)00105-7.

[13] Schoenholz C, Slade D, Zappino E, Petrolo M, Zobeiry N. Representation, Characterization and Simulation of Tool-Part Interaction and Its Effects on Process-Induced Deformations in Composites. Proceedings of the American Society for Composites—Thirty-Sixth Technical Conference on Composite Materials, vol. 0, DEStech Publications; 2021, p. 1204–16. https://doi.org/10.12783/ASC36/35832.

[14] Schoenholz C, Moomaw J, Zobeiry N. Investigating the Effects of Cure Pressure on Tool-Part Interaction and Process-Induced Deformations in Composites. PROCEEDINGS OF THE AMERICAN SOCIETY FOR COMPOSITES-THIRTY-SEVENTH TECHNICAL CONFERENCE, vol. 0, DEStech Publications Inc.; 2022. https://doi.org/10.12783/ASC37/36383.

[15] Stefaniak D, Kappel E, Spröwitz T, Hühne C. Experimental identification of process parameters inducing warpage of autoclave-processed CFRP parts. Compos Part A Appl Sci Manuf 2012;43:1081–91. https://doi.org/10.1016/J.COMPOSITESA.2012.02.013.

[16] Schoenholz C, Li S, Bainbridge K, Huynh V, Gray A, Chen X, et al. An Automated Evaluation Method of Tool Surface Condition in Composites Manufacturing Using Machine Learning and Sparse Sensing. SAMPE Journal: Tooling Technology Advancement/Applications 2023;59:10–23.

[17] Bainbridge K, Schoenholz C, Zobeiry N. Investigating the aging of release coating in aerospace composites manufacturing. University of Washington Undergraduate Research in MSE 2021;2:7–11. https://doi.org/10.6069/ssywg443.

[18] Zobeiry N, Gray A, Bainbridge K, Li S, Huynh V, Chen X, et al. A Machine Learning-Based Portable Inspection Method for Evaluation of Tool Surface Condition and Release Coating in Composites Manufacturing. SAMPE 2022 2022. https://doi.org/10.33599/NASAMPE/S.22.0740.

[19] Blass D, Dilger K. CFRP-Part Quality as the Result of Release Agent Application – Demoldability, Contamination Level, Bondability. Procedia CIRP, vol. 66, Elsevier; 2017, p. 33–8. https://doi.org/10.1016/J.PROCIR.2017.03.219.

[20] Critchlow GW, Litchfield RE, Sutherland I, Grandy DB, Wilson S. A review and comparative study of release coatings for optimised abhesion in resin transfer moulding applications. Int J Adhes Adhes 2006;26:577–99. https://doi.org/10.1016/J.IJADHADH.2005.09.003.

[21] LOCTITE FREKOTE 710NC - Release Agent - Henkel Adhesives 2015. https://www.pccomposites.com/product/frekote-710nc/ (accessed September 1, 2022).

[22] Markatos DN, Tserpes KI, Rau E, Markus S, Ehrhart B, Pantelakis S. The effects of manufacturing-induced and in-service related bonding quality reduction on the mode-I fracture toughness of composite bonded joints for aeronautical use. Compos B Eng 2013;45:556–64. https://doi.org/10.1016/J.COMPOSITESB.2012.05.052.

[23] 3900 Prepreg System | Toray Composite Materials America, Inc. 2020. https://www.toraycma.com/3900-prepreg-system/ (accessed September 1, 2022).

[24] Brosius D. Boeing 787 Update. CompositesWorld 2007. https://www.compositesworld.com/articles/boeing-787-update (accessed November 13, 2022).

[25] Steel Feeler Gage 1/2" x 12" Blades - Precision Brand n.d. https://www.precisionbrand.com/product-category/1-2-x-12-blades-steel-feeler-gage/ (accessed December 28, 2022).
[26] ISO - ISO 1302:2002 - Geometrical Product Specifications (GPS) — Indication of surface texture in technical product documentation 2002. https://www.iso.org/standard/28089.html (accessed September 28, 2022).
[27] LOCTITE FREKOTE PMC - solvent-based post mould cleaner - Henkel Adhesives n.d. https://www.henkel-adhesives.com/us/en/product/mold-release-cleaners/loctite_frekote_pmc.html (accessed December 28, 2022).
[28] Owens DK, Wendt RC. Estimation of the surface free energy of polymers. J Appl Polym Sci 1969;13:1741–7. https://doi.org/10.1002/APP.1969.070130815.
[29] FlexiForce HT201 Sensor | Tekscan n.d. https://www.tekscan.com/products-solutions/force-sensors/ht201 (accessed December 28, 2022).
[30] de Gennes P-G, Brochard-Wyart F, Quéré D. Capillarity and Wetting Phenomena. Springer New York; 2004. https://doi.org/10.1007/978-0-387-21656-0.
[31] Persson BNJ. On the theory of rubber friction. Surf Sci 1998;401:445–54. https://doi.org/10.1016/S0039-6028(98)00051-X.
[32] Wenzel RN. Surface roughness and contact angle. Journal of Physical & Colloid Chemistry 1949;53:1466–7. https://doi.org/10.1021/J150474A015/ASSET/J150474A015.FP.PNG_V03.
[33] Chen C, Poursartip A, Fernlund G. Cure-dependent microstructures and their effect on elastic properties of interlayer toughened thermoset composites. Compos Sci Technol 2020;197:108241. https://doi.org/10.1016/J.COMPSCITECH.2020.108241.
[34] Otsuki M, Matsukawa H. Systematic Breakdown of Amontons' Law of Friction for an Elastic Object Locally Obeying Amontons' Law. Scientific Reports 2013 3:1 2013;3:1–6. https://doi.org/10.1038/srep01586.